

Enhancement of rectification by quantum interference in co-oligomer molecular diodes

Han-Shuang Zhang(张含双), Han Ma(马晗), Hui-Qing Zhang(张惠晴), Xiao-Bei Zhang(张晓蓓), Jun-Feng Ren(任俊峰), Guang-Ping Zhang(张广平), and Gui-Chao Hu(胡贵超)
Citation: Chin. Phys. B, 2026, 35 (**4**): 048504. DOI: 10.1088/1674-1056/ae0b3d
http://cpb.iphy.ac.cn; http://iopscience.iop.org/cpb

What follows is a list of articles you may be interested in

Increasing linear flux range of SQUID amplifier using self-feedback effect

Ying-Yu Chen(陈滢宇), Chao-Qun Wang(王超群), Yuan-Xing Xu(徐元星), Yue Zhao(赵越), Li-Liang Ying(应利良), Hang-Xing Xie(谢颃星), Bo Gao(高波), and Zhen Wang(王镇)
Chin. Phys. B, 2023, 32 (**11**): 118501. DOI: 10.1088/1674-1056/acd8ac

Designing current-strain-assisted superconductor-ferromagnet multi-bit memories

Hasnain Mehdi Jafri, Jing Wang(王静), Xiao-Ming Shi(施小明), De-Shan Liang(梁德山), and Hou-Bing Huang(黄厚兵)
Chin. Phys. B, 2022, 31 (**11**): 118501. DOI: 10.1088/1674-1056/ac7e36

Multiplexing technology based on SQUID for readout of superconducting transition-edge sensor arrays

Xinyu Wu(吴歆宇), Qing Yu(余晴), Yongcheng He(何永成), Jianshe Liu(刘建设), and Wei Chen(陈炜)
Chin. Phys. B, 2022, 31 (**10**): 108501. DOI: 10.1088/1674-1056/ac693c

Development of series SQUID array with on-chip filter for TES detector

Wentao Wu(伍文涛), Zhirong Lin(林志荣), Zhi Ni(倪志), Peizhan Li(李佩展), Tiantian Liang(梁恬恬), Guofeng Zhang(张国峰), Yongliang Wang(王永良), Liliang Ying(应利良), Wei Peng(彭炜), Wen Zhang(张文), Shengcai Shi(史生才), Lixing You(尤立星), and Zhen Wang(王镇)
Chin. Phys. B, 2022, 31 (**2**): 028504. DOI: 10.1088/1674-1056/ac2b91

Reversible waveform conversion between microwave and optical fields in a hybrid opto-electromechanical system

Li-Guo Qin(秦立国), Zhong-Yang Wang(王中阳), Jie-Hui Huang(黄接辉), Li-Jun Tian(田立君), and Shang-Qing Gong(龚尚庆)
Chin. Phys. B, 2021, 30 (**6**): 068502. DOI: 10.1088/1674-1056/abea8f

---

Enhancement of rectification by quantum interference in co-oligomer molecular diodes

Han-Shuang Zhang(张含双), Han Ma(马晗), Hui-Qing Zhang(张惠晴), Xiao-Bei Zhang(张晓蓓), Jun-Feng Ren(任俊峰), Guang-Ping Zhang(张广平)†, and Gui-Chao Hu(胡贵超)‡

School of Physics and Electronics, Shandong Normal University, Jinan 250358, *China*

(Received 5 August 2025; revised manuscript received 13 September 2025; accepted manuscript online 25 September 2025)

We investigate the rectification property theoretically in co-oligomer diodes integrating a destructive quantum interference (DQI) feature. The results demonstrate that compared to a similar co-oligomer diode without DQI, the rectification ratio is enhanced by one order of magnitude in the presence of the DQI feature. Mechanism analysis indicates that the high rectification ratio benefits from the strong suppression of transmission in the off-state of the diode by the DQI dip. The strong rectification is attributed to the distinctly asymmetric shift of the DQI dip under bias voltages, which comes out as a result of both bias-induced shift of eigenvalues and redistribution of wave functions of all orbitals. The effect of energy level alignment between the two segments of the co-oligomer on the rectification is also discussed. This work provides a valid way to enhance the performance of intrinsic co-oligomer diodes, a promising approach for molecular circuit design.

Keywords: quantum interference, molecular rectification, co-oligomer

PACS: 85.65.+h, 72.80.Le, 73.23.–b

DOI: 10.1088/1674-1056/ae0b3d **CSTR:** 32038.14.CPB.ae0b3d

1. Introduction

Quantum interference (QI) effect is an efficient way to modulate electron transport properties through molecular junctions,[1–5] which originates from the interference among the one-electron wave functions propagating through different molecular orbitals. The typical example is that in meta-linked benzene junctions, the electron transmission around the Fermi energy is strongly suppressed known as destructive quantum interference (DQI).[6] Currently, the QI effect has been confirmed experimentally in various π-conjugated systems, ranging from benzene derivatives[7–10] to polycyclic aromatic hydrocarbons,[11–13] diarylethenes,[14,15] cyclophanes,[16–18] and polyenes.[19,20] Even in σ-systems the QI effect was also observed.[21] Due to the strong suppression of conductance, in molecular electronics the DQI has been utilized to design molecular switches,[22] molecular spin filters,[23] and molecular thermoelectric devices.[24,25] The exploration of the role of DQI in various molecular functional devices remains attractive.

Molecular diodes are one of the fundamental elements in molecular electronics. Since they were proposed by Aviram and Ratner in 1974,[26] various molecular diodes have been designed and examined.[27–32] Particularly, diblock donor-acceptor co-oligomer molecular diodes, such as dipyrimidinyl–diphenyl co-oligomers, have gained enormous attention known as intrinsic molecular diodes.[31] The rectification in such diodes is caused by the intrinsic structural asymmetry, and so the diodes are promising to be designed in molecular circuits. However, the rectification ratio (RR) in co-oligomer diodes is not large enough in most experimental reports (on the order of 10),[33,34] which limits the future application in molecular electronics. A basic reason for the small RR is that although a larger barrier usually holds in the off-state, the leak current cannot be blocked completely for a single molecule in the case of tunneling, which sets up a barrier for the future application of co-oligomer diodes in spite of the advantage in integration of molecular circuits.

The DQI effect is a valid way to achieve ultra-low conductance. However, the application of DQI in molecular diodes is challenged by the realization of an asymmetric response to the bias voltage for the DQI dip. In this work, we construct a co-oligomer diode consisting of an anthracene molecule and a polyacetylene chain. The DQI feature is integrated by setting a meta connection of the anthracene molecule. It is found that a large rectification is realized, where the transmission in the off-state is strongly suppressed by the DQI dip. In contrast with the counterpart without DQI, the RR is enhanced by one order of magnitude. The paper is organized as follows. In Section 2, the model and calculation method are introduced. In Section 3, the numerical calculations are carried out and the results are analyzed. A brief summary is given in Section 4.

†Corresponding author. E-mail: zhangguangping@sdnu.edu.cn

‡Corresponding author. E-mail: hgc@sdnu.edu.cn

© 2026 Chinese Physical Society and IOP Publishing Ltd. All rights, including for text and data mining, AI training, and similar technologies, are reserved.

2. Model and method

The model structure of the co-oligomer diode is shown in Fig. 1, which consists of the left anthracene and the right polyacetylene oligomers. The co-oligomer is connected to two one-dimensional nonmagnetic metals via the terminal sites. For the left electrode, we consider two different connection sites on the anthracene here. One is on the upper terminal site to form a para connection for the anthracene molecule by the electrode and the polyacetylene in Fig. 1(a), where the DQI will be absent. The other is on the lower terminal site and thus a meta connection is formed in Fig. 1(b), where the DQI will be expected. Since the left anthracene molecule can be viewed as two coupled polyacetylene chains, the whole co-oligomer in Fig. 1 is composed of two coupled chains with unequal length. The co-oligomer is described by an extended Su–Schrieffer–Heeger (SSH) model with the as[35,36]

$$H = \sum_j H_j + H_{\rm c} + H_E. \tag{1}$$

Here, H_j denotes the Hamiltonian of a single chain

$$H_j = \sum_i \varepsilon_0 c^{\dagger}_{i,j} c_{i,j} - \sum_i t_{i,j}(c^{\dagger}_{i+1,j} c_{i,j} + {\rm H.c.}) + \frac{1}{2} K \sum_i y^2_{i,j}. \tag{2}$$

The first term is the on-site energy of co-oligomer sites relative to electrodes. The second term denotes the nearest π-electron hopping along the jth chain ($j = 1,\ 2$) with $t_{i,j} = t_0 - \alpha y_{i,j}$. α is the electron–lattice (e-l) coupling constant, and $y_{i,j}$ represents the lattice distortion, defined as $y_{i,j} = u_{i+1,j} - u_{i,j}$ with $u_{i,j}$ the displacement of the carbon atom at the ith site of the jth chain. $c^{\dagger}_{i,j}$ ($c_{i,j}$) represents the creation (annihilation) operator for an electron that is created (annihilated) at the ith site of the jth chain. The third term represents the elastic energy of the lattice, characterized by the elastic coefficient K.

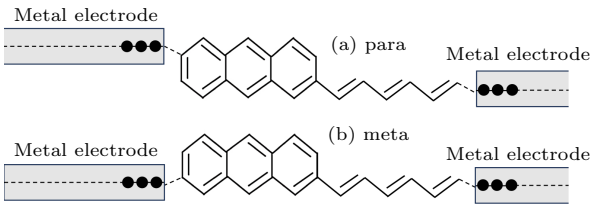


Fig. 1. Simplified structure of the co-oligomer diode (a) with para and (b) meta connections of the left electrode.

The $H_{\rm c}$ denotes the Hamiltonian associated with the interchain hopping of the π-electrons, which only exists in the left anthracene molecule and can be written as

$$H_{\rm c} = -\sum_i^{N_1} t_1 \delta_{i,{\rm odd}} (c^{\dagger}_{i,1} c_{i,2} + {\rm H.c.}). \tag{3}$$

Here, t_1 is the interchain hopping integral, which occurs only at odd sites of the chain with $\delta_{i,{\rm odd}} = 1$ ($\delta_{i,{\rm odd}} = 0$) for odd (even) atoms. N_1 represents the total number of sites in chain 1, that is, the upper chain in the anthracene molecule ($j = 1$).

The H_E represents the Hamiltonian of potential related to the spatial electric field E generated by the external bias voltage V

$$\begin{aligned} H_E \ =\ & -\sum_{i,j} eE[(i - N_1)a + u_{i,j}] c^{\dagger}_{i,j} c_{i,j} \\ & + \sum_{i,j} eE[(i - N_1)a + u_{i,j}]. \end{aligned} \tag{4}$$

The first term represents the electric potential of π electrons, and the second term is for the lattice ions. e is the elementary charge and a is the lattice constant along each chain. The electric field E is related to the bias voltage V as $E = V/[(N_2 - 1)a]$ with N_2 the total site number of the lower chain ($j = 2$). The use of the linear electric field for electric potential is valid when the bias voltage is not too large.[37]

The stable state of the molecule is obtained by solving the electronic eigen equations and lattice equilibrium equations self-consistently. The electronic eigenvalue equations are expressed as

$$\varepsilon_\mu Z_{\mu,i,j} = -t_{i,j} Z_{\mu,i+1,j} - t_{i-1,j} Z_{\mu,i-1,j} - t_1 \delta_{i,{\rm odd}} Z_{\mu,i,j\pm1}. \tag{5}$$

Here, ε_μ and $Z_{\mu,i,j}$ are the eigenenergy and the eigenfunction in Wannier space, respectively. The lattice equilibrium equation is written as

$$\begin{aligned} y_{i,j} \ =\ & -\frac{2\alpha}{K} \sum_{\mu,{\rm occ}} Z_{\mu,i,j} Z_{\mu,i+1,j} \\ & + \frac{2\alpha}{(N_j - 1)K} \sum_{i=1}^{N_j - 1} \sum_{\mu,{\rm occ}} Z_{\mu,i,j} Z_{\mu,i+1,j} \\ & - \frac{|e|E}{K} \sum_{\mu,{\rm occ}} Z_{\mu,i,j} Z_{\mu,i,j} \\ & + \frac{|e|E}{(N_j - 1)K} \sum_{i=1}^{N_j - 1} \sum_{\mu,{\rm occ}} Z_{\mu,i,j} Z_{\mu,i,j}. \end{aligned} \tag{6}$$

In our calculation, fixed-end boundary conditions are adopted with $u_{1,j} = u_{N_j,j} = 0$. Equations (5) and (6) need to be solved iteratively, until a self-consistent solution is reached, that is, the variation of $|y_{i,j}|$ between two steps is less than 10^{-6} Å.

The electrodes are described with a single-band tight-binding model with hopping integral $t_{\rm f}$. The interfacial coupling between the electrodes and the co-oligomer is simplified as a transfer integral $t_{\rm mf} = \beta(t_0 + t_{\rm f})/2$. β is the weight parameter.

Applying a bias voltage V, the stable state of the co-oligomer under the electric field can be calculated by solving the electronic eigen equations and lattice equilibrium equations self-consistently.[38,39] After that, the current of the device at a bias voltage will be calculated with the Landauer–Büttiker formula[40]

$$I = \frac{2e}{h} \int_{-\infty}^{+\infty} T(E)[f(E - \mu_{\rm L}) - f(E - \mu_{\rm R})]\,{\rm d}E. \tag{7}$$

Here $T(E)$ represents the transmission spectrum at energy E, which is given by $T(E) = {\rm Tr}\left[\Gamma_{\rm L} G(E) \Gamma_{\rm R} G^{\dagger}(E)\right]$. $\Gamma_{p({\rm p=L,R})}$ is

the coupling matrix between the p-th electrode and the co-oligomer with $\Gamma_p = \mathrm{i}[\Sigma_p - \Sigma_p^+]$. Σ_p refers to the self energy induced by the coupling with the p-th electrode, which can be calculated from $\Sigma_p = t_{\mathrm{mf}}^+ g_p t_{\mathrm{mf}}$. g_p is the surface Green's function of the p-th electrode. $G(E)/G^\dagger(E)$ is the retarded/advanced Green's function of the central co-oligomer. $f(E-\mu_{\mathrm{L/R}})$ represents the Fermi–Dirac distribution function with chemical potential of the left/right electrode $\mu_{\mathrm{L/R}} = E_{\mathrm{F}} \pm \frac{eV}{2}$ and Fermi energy E_{F}.

For the numerical simulations, we take the parameters referring to those of polyacene and polyacetylene:[41] $t_0 = t_1 = 2.5$ eV, $\alpha = 4.5$ eV/Å, $K = 21.0$ eV/Å^2, $\varepsilon_0 = 0.5$ eV, $N_1 = 7$, and $N_2 = 13$. The proposed model should be valid for other co-oligomers with a similar structure. The parameters of the electrode are taken as $t_{\mathrm{f}} = 1.5$ eV, $E_{\mathrm{F}} = 0$. The interfacial binding parameter is $\beta = 0.5$.

3. Results and discussion

We start from the current–voltage characteristics of the co-oligomer diodes with different connections. As shown in Figs. 2(a) and 2(b), the rectification behavior is observed in both asymmetric junctions, where the current in the positive bias region is much larger than that in the negative bias region. The largest current in the positive bias region of the two junctions exceeds 4.0 μA. In the negative bias region, a finite current of about 0.64 μA remains at −0.95 V for the para-connection junction. However, in the case of the meta-connection junction, the current is strongly suppressed (<0.1 μA), which leads to a more pronounced rectification. By defining the bias-dependent RR as $RR(V) = I(+V)/I(-V)$, we calculate the RR at every bias voltage and give the results in Figs. 2(c) and 2(d). The largest RR for the para-connection junction is 5.65 at 0.95 V, which is comparable to that in the experiments of other co-oligomer diodes, such as thiophene-thiazole[29] and dipryrimidinyl-diphenyl.[42] However, for the meta-connection junction, it is noticed that the largest RR achieves 53 at 0.95 V, which is ten times of the para-connection junction.

To understand the underlying mechanism of rectification, we first investigate the transmission spectrum at different bias voltages, as shown in Fig. 3. For the para-connection co-oligomer diode, there is no DQI feature around the Fermi energy, and the conducting transmission is mainly contributed by the peak from the highest occupied molecular orbital (HOMO). The rectification is induced by the asymmetric shift of the HOMO peak, which moves closer to the Fermi energy at the positive bias and farther away from the Fermi energy at the negative bias. The asymmetric shift of conducting states is a common mechanism for rectification widely reported in co-oligomer diodes,[43–45] caused by the bias effect on the asymmetrically distributed frontier molecular orbitals. For the meta-connection co-oligomer diode at zero bias, an expected distinct DQI dip appears at 0.5 eV between the HOMO and LUMO (lowest unoccupied molecular orbital) peaks, where the magnitude of transmission is suppressed to the order of 10^{-8}. Applying a bias voltage, the DQI dip also moves asymmetrically, similar to molecular orbitals. As a result, the DQI dip locates in the bias window at −0.9 V and out of the bias window at 0.9 V. Thus, the tunneling current at the negative bias is strongly suppressed by the DQI dip, which enhances the rectification significantly.

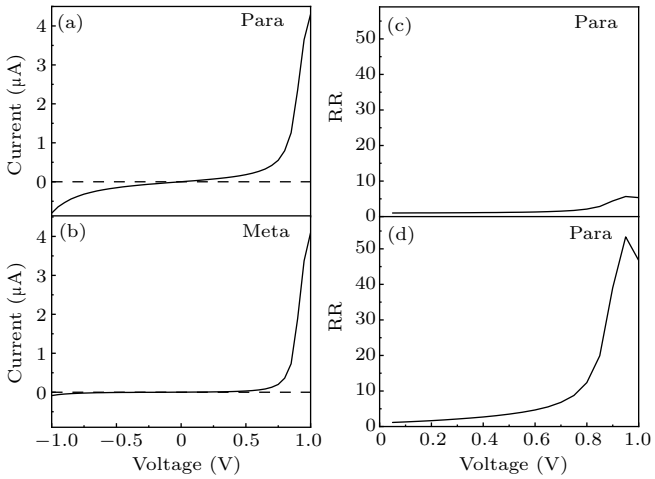


Fig. 2. Current–voltage curve and rectification ratio of co-oligomer molecular diodes: (a) and (c) para connection without quantum interference effect, (b) and (d) meta connection with quantum interference effect.

The DQI feature in the co-oligomer diode can be further confirmed by the wave functions of frontier molecular orbitals. It is known that the DQI dip in the transmission spectrum is caused by the destructive interference between different conducting orbitals, which can be roughly analyzed using Green's functions.[12] For the DQI dip around the Fermi energy, although in nature it comes out as the result of interference between all molecular orbitals, the HOMO and LUMO orbitals play a dominant role as adjacent states in energy. The Green's function is usually defined as $G(E) = \frac{1}{E-H-\sum_p \Sigma_p + \mathrm{i}\eta}$ with η the infinitesimal. The transmission is related to the Green's function at the two terminal sites of the molecule. By expanding Green's function in Wannier representation and neglecting the slight correction from the self-energy term, the Green's function for the two terminal sites can be expressed as[11,12] [46]

$$G_{\mathrm{LR}}(E) \sim \sum_k \frac{C_{\mathrm{L},k} C_{\mathrm{R},k}^*}{E-\varepsilon_k} \approx \frac{C_{\mathrm{L,HOMO}} C_{\mathrm{R,HOMO}}^*}{E-\varepsilon_{\mathrm{HOMO}}} + \frac{C_{\mathrm{L,LUMO}} C_{\mathrm{R,LUMO}}^*}{E-\varepsilon_{\mathrm{LUMO}}}. \tag{8}$$

In the above equation, $C_{\mathrm{L/R},k}$ denotes the coefficient of the kth molecular orbital at the coupling site of the molecule by the left/right electrode. ε_k is the eigenvalue of the kth orbital. Since the LUMO and HOMO are the nearest orbitals to the dip, the value of Green's function is mainly determined by the

two orbitals (at least at zero bias). The eigen value ε_k and coefficient $C_{\mathrm{L/R},k}$ can be obtained from the electronic eigen equations at each bias voltage. To form the DQI dip, one needs $G_{\mathrm{LR}}(E) \to 0$ and thus the signs of the two terms in Eq. (8) should be opposite. The wave functions of the co-oligomers at different bias voltages are given in Fig. 4. For the meta-connection diode, the signs of the wave functions at the left and right coupling sites keep opposite for both the HOMO and LUMO, either under zero or nonzero bias voltage, which eventually induce a zero point of Green's function at some energy between $\varepsilon_{\mathrm{HOMO}}$ and $\varepsilon_{\mathrm{LUMO}}$ near the Fermi energy. But for the para-connection diode, we find that the signs of the wave functions of the HOMO at the two coupling sites are the same, where the two terms in Eq. (8) have the same sign and lead to constructive interference.

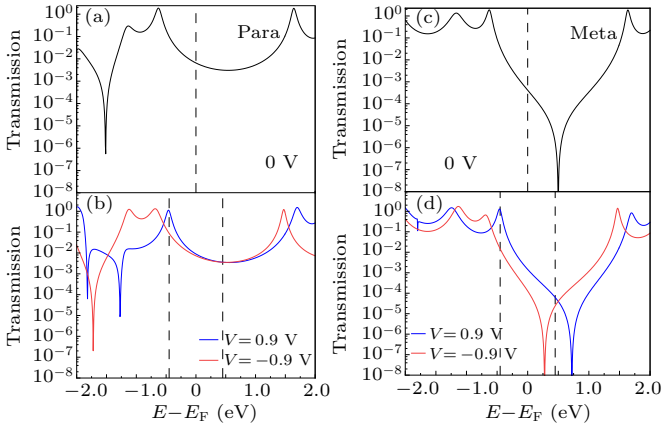


Fig. 3. Transmission coefficients near the Fermi energy at $V = 0$ V, 0.9 V and −0.9 V: (a) and (b) para connection, (c) and (d) meta connection. The dashed lines indicate the bias window.

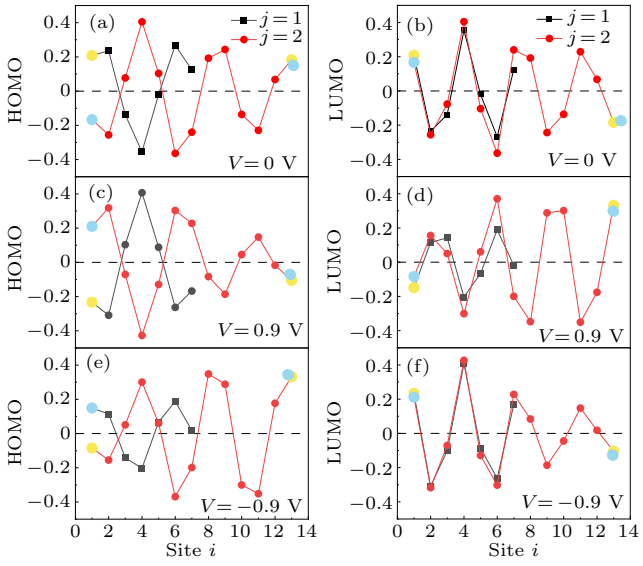


Fig. 4. Wave functions of the HOMO and LUMO at different bias voltages. The yellow (blue) dots indicate the coupled sites by electrodes of para (meta) connection.

From Fig. 3, one can find that another point benefiting for a stronger rectification in the meta-connection diode is that the asymmetric shift of the DQI dip under bias voltage is larger than that of conjugated molecular orbitals. For example, the energy difference between 0.9 V and −0.9 V is about 0.5 eV for the DQI dip, while it is less than 0.2 eV for the HOMO and LUMO. In the following, we calculate the bias-induced shift of the HOMO, LUMO and DQI dip relative to the zero bias voltage, respectively. Here, the exact position of the DQI dip at each bias voltage is determined numerically by solving the equation $G_{\mathrm{LR}}(E) \sim \sum_k \frac{C_{\mathrm{L},k} C^*_{\mathrm{R},k}}{E-\varepsilon_k} = 0$ for all eigen states. As shown in Fig. 5, it is found that the HOMO and LUMO are lifted by positive bias voltage and lowered by negative bias voltage. This is because the two frontier orbitals mainly distribute in the left anthracene moiety due to its smaller energy gap, which will be lifted (lowered) by the electric potential from the positive (negative) bias voltage. The shifted quantity of the HOMO and LUMO is asymmetric under positive and negative bias voltages, which is caused by the bias-dependent orbital hybridization of the co-oligomer.[30,43] Unlikely, the shift of the DQI dip looks almost linear and symmetric under bias voltages. Especially, the magnitude of the shift is larger than the HOMO and LUMO at every bias voltage.

The large energy shift of the DQI dip can be understood as follows. From Eq. (8), the corresponding energy of the DQI dip, that is, the zero-point energy of $G_{\mathrm{LR}}(E) = \sum_k \frac{C_{\mathrm{L},k} C^*_{\mathrm{R},k}}{E-\varepsilon_k} = 0$, is codetermined by both the eigenvalues and wave functions at coupling sites. For co-oligomers diodes, besides the energy shift of eigenvalues, the spatial distribution of wave functions is also significantly modulated by bias voltages.[30,43] As a result, the coefficients on the coupling sites of each eigenstate depend on the bias voltage. For example, such evolution can be clearly seen in Fig. 4 for the HOMO and LUMO. The product of coefficients at the coupling sites changes from −0.030 (−0.030) at 0 V to −0.022 (−0.028) at 0.9 V, and to −0.028 (−0.022) at −0.9 V for the HOMO (LUMO). Additionally, we also find that as the bias voltage is increased, the position of the DQI dip further away from the position calculated using only the HOMO and LUMO, which means the contribution to the DQI from other orbitals is enhanced.

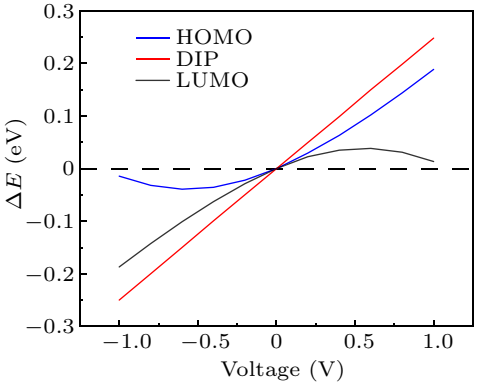


Fig. 5. The energy difference, defined as $\Delta E = E_V - E_{V=0}$, as a function of the bias voltage for the HOMO, LUMO and DQI dip.

In the present designed co-oligomer diodes, the HOMO and LUMO are mainly contributed by the left moiety. In general, the two orbitals of co-oligomers may be located in different moieties, such as a donor/acceptor structure, where the bias-induced energy shift of HOMO and LUMO will be opposite. In reality, the energy level alignment between the two segments of co-oligomers can be controlled during chemical synthesis by changing the types of oligomers with different electron affinities and ionization energies. To generalize our proposed physics, we further examined the DQI effect on the rectification in that case. For simplicity, here we modify the on-site energies of each atom in the left moiety of the co-oligomer as $\varepsilon_{\mathrm{L}} = 0.6$ eV and in the right one as $\varepsilon_{\mathrm{R}} = -0.5$ eV. Thus, the HOMO is located in the left moiety and the LUMO in the right moiety. The calculated current–voltage curve and bias-induced shift of orbitals are shown in Fig. 6. Compared with the para connection, the significant enhancement of RR in the case of meta connection is still observed, where the maximum RR increases from 4 to 209. Figure 6(b) demonstrates an opposite shift for the HOMO and LUMO at each bias voltage, due to their different localization in the two moieties. However, a similar linear shift as in theabove case is obtained for the DQI dip, where the magnitude is close to the HOMO.

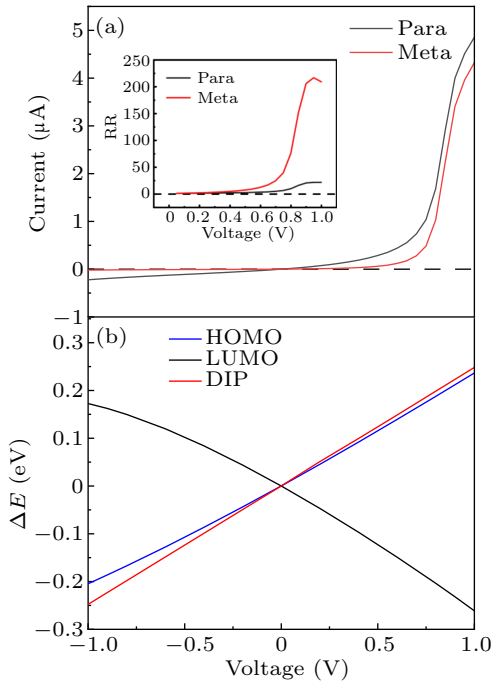


Fig. 6. (a) Current–voltage curves for co-oligomer diodes where the HOMO and LUMO are located in different moieties. The inset is the rectification ratio. (b) Bias-induced energy shift for the HOMO, LUMO and DQI dip.

We further investigate the dependence of the RR on the difference of on-site energies between the two segments. Here we use the parameters as those in Fig. 2, except that the on-site energy of the right segment is modified as $\varepsilon_{\mathrm{R}} = \varepsilon + \Delta\varepsilon$. The RR at 0.95 V is calculated with the variation of $\Delta\varepsilon$. As shown in Fig. 7, it is found that the RR shows a nonlinear dependence on $\Delta\varepsilon$. When $\Delta\varepsilon$ is less than 0.4 eV, the RR decreases with the increase of $\Delta\varepsilon$, reaching about 15 at $\Delta\varepsilon = 0.4$ eV. Beyond that, the RR increases with $\Delta\varepsilon$. The reason is that the rectification is mainly contributed by the asymmetric shift of the DQI dip and the transmission tail of the HOMO state. When $\Delta\varepsilon$ is less than 0.4 eV, the HOMO mainly locates in the left segment. If $\Delta\varepsilon$ turns smaller, the electronic localization of the HOMO state becomes stronger, which leads to a larger asymmetric energy shift of the HOMO under bias voltages, and so benefits a larger RR. The electronic localization of the HOMO state is the smallest at $\Delta\varepsilon = 0.4$ eV, corresponding to the smallest value of RR. Beyond that, the HOMO state is located in the right segment, whose electronic localization will be enhanced with the increase of $\Delta\varepsilon$, as well as the RR.

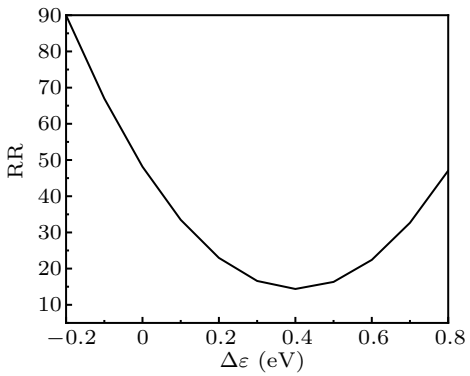


Fig. 7. The variation of RR at 0.95 V with the change of on-site energy in the right segment.

The proposed co-oligomer diodes with DQI feature are expected to be examined easily in experiments using the scanning tunneling microscope break junction[7] or the mechanically controllable break junction technique.[47] To amplify the role of the DQI effect, a deep DQI dip adjacent to the Fermi energy is preferred. This can be achieved in experiments by tuning the position of the dip via heteroatom substitution,[48,49] or by using suitable electrode species. Recently, a single-molecule diode with high RR based on the DQI effect has been reported,[50] where the molecule may switch between a structure with CQI and a structure with DQI, triggered by the electric field. Instead, our proposed co-oligomer diodes with the DQI work without a structure transition, and can be integrated into a molecular circuit.

4. Conclusion

In summary, we have investigated the role of DQI effect on the rectification in intrinsic co-oligomer molecular diodes. The appearance of the DQI feature is controlled by changing the coupling sites of the electrode to form a para or meta connection. The results demonstrate that compared with the normal co-oligomer diodes, the RR in the diodes integrating the DQI feature is enhanced by one order of magnitude.

The mechanism analysis indicates that the large RR originates from the strong suppression of the transmission by the DQI dip at a negative bias voltage. The high-performance rectification also benefits from the distinctly asymmetric shift of the DQI dip under bias voltage, which is caused by both the bias-induced energy shift of molecular eigenvalues and the redistribution of wave functions. This work proposes a strategy to enhance the performance of intrinsic co-oligomer diodes, which deserves to be tested in experiments.

Acknowledgements

Project supported by the Shandong Provincial Natural Science Foundation (Grant No. ZR2025MS09), the National Natural Science Foundation of China (Grant Nos. 12474212 and 12274264), and the China Scholar Council.

References

[1] Hong W J, Valkenier H, Mészáros G, Manrique D Z, Mishchenko A, Putz A, García P M, Lambert C J, Hummelen J C and Wandlowski T 2011 *Beilstein J. Nanotechnol.* **2** 699
[2] Guédon C M, Valkenier H, Markussen T, Thygesen K S, Hummelen J C and van der Molen S J 2012 *Nat. Nanotech.* **7** 305
[3] Mayor M, Weber H B, Reichert J, Elbing M, von Hänisch C, Beckmann D and Fischer M 2003 *Angew. Chem. Int. Ed.* **42** 5834
[4] Cardamone D M, Stafford C A and Mazumdar S 2006 *Nano Lett.* **6** 2422
[5] Solomon G C, Andrews D Q, Goldsmith R H, Hansen T, Wasielewski M R, Van Duyne R P and Ratner M A 2008 *J. Am. Chem. Soc.* **130** 17301
[6] Sautet P and Joachim C 1988 *Chem. Phys. Lett.* **153** 511
[7] Kiguchi M, Nakamura H, Takahashi Y, Takahashi T and Ohto T 2010 *J. Phys. Chem. C* **114** 22254
[8] Yang G G, Wu H, Wei J Y, Zheng J T, Chen Z B, Liu J Y, Shi J, Yang Y and Hong W J 2018 *Chin. Chem. Lett.* **29** 147
[9] Stadler R 2009 *Phys. Rev. B* **80** 125401
[10] Manrique D Z, Huang C, Baghernejad M, Zhao X T, Al-Owaedi O A, Sadeghi H, Kaliginedi V, Hong W J, Gulcur M, Wandlowski T, Bryce M R and Lambert C J 2015 *Nat. Commun.* **6** 6389
[11] Yoshizawa K 2012 *Acc. Chem. Res.* **45** 1612
[12] Zhao X, Geskin V and Stadler R 2018 *J. Chem. Phys.* **146** 092308
[13] Tsuji Y and Hoffmann R 2014 *Angew. Chem. Int. Ed.* **53** 4093
[14] Tsuji Y, Staykov A and Yoshizawa K 2009 *J. Phys. Chem. C* **113** 21477
[15] Reecht G, Lotze C, Sysoiev D, Huhn T and Franke K J 2016 *Acs Nano* **10** 10555
[16] Tsuji Y, Okazawa K, Kurino K and Yoshizawa K 2022 *J. Phys. Chem. C* **126** 3244
[17] Chen H L, Hou S J, Wu Q Q, Jiang F, Zhou P, Zhang L, Jiao Y, Song B, Guo Q H, Chen X Y, Hong W J, Lambert C J and Stoddart J F 2021 *Matter* **4** 3662
[18] Schosser W M, Hsu C W, Zwick P, Beltako K, Dulic D, Mayor M, van der Zant H S J and Pauly F 2022 *Nanoscale* **14** 984
[19] Gu J J, Wu W, Stuyver T, Danovich D, Hoffmann R, Tsuji Y and Shaik S 2019 *J. Am. Chem. Soc.* **141** 6030
[20] Tsuji Y, Hoffmann R, Movassagh R and Datta S 2014 *J. Chem. Phys.* **141** 224311
[21] Tsuji Y, Okazawa K, Tatsumi T and Yoshizawa K 2024 *J. Am. Chem. Soc.* **146** 32506
[22] Greenwald J E, Cameron J, Findlay N J, Fu T, Gunasekaran S, Skabara P J and Venkataraman L 2021 *Nat. Nanotech.* **16** 313
[23] Pal A N, Li D, Sarkar S, Chakrabarti S, Vilan A, Kronik L, Smogunov A and Tal O 2019 *Nat. Commun.* **10** 5565
[24] Hu S T, Qian M, Zhang G and Zhang B 2025 *Chin. Phys. B* **34** 068903
[25] Zhang B, Zhang S D and Long M Q 2022 *Phys. E* **139** 115189
[26] Aviram A and Ratner M A 1974 *Chem. Phys. Lett.* **29** 277
[27] Ng M K, Lee D C and Yu L P 2002 *J. Am. Chem. Soc.* **124** 11862
[28] Elbing M, Ochs R, Koentopp M, Fischer M, von Hänisch C, Weigend F, Evers F, Weber H B and Mayor M 2005 *Proc. Natl. Acad. Sci. USA* **102** 8815
[29] Jiang P, Morales G M, You W and Yu L 2004 *Angew. Chem. Int. Ed.* **43** 4471
[30] Hu G C, Wei J H and Xie S J 2007 *Appl. Phys. Lett.* **91** 142115
[31] Ma J, Yang C L, Wang L Z, Wang M S and Ma X G 2014 *Physica B* **434** 32
[32] Zhang P P, Tan S H, Peng X F and Long M Q 2020 *Chin. Phys. B* **29** 106801
[33] Morales G M, Jiang P, Yuan S W, Lee Y G, Sanchez A, You W and Yu L P 2005 *J. Am. Chem. Soc.* **127** 10456
[34] Kushmerick J G, Whitaker C M, Pollack S K, Schull T L and Shashidhar R 2004 *Nat. Nanotech.* **15** S489
[35] Su W P, Schrieffer J R and Heeger A J 1979 *Phys. Rev. Lett.* **42** 1698
[36] Miao Y Y, Chen L Y, Zhang G P, Wang C K, Ren J F, Timm C and Hu G C 2022 *Phys. Rev. B* **105** 094419
[37] Mujica V, Roitberg A E and Ratner M 2000 *J. Chem. Phys.* **112** 6834
[38] Hu G C, Zuo M Y, Li Y, Ren J F and Xie S J 2014 *Appl. Phys. Lett.* **104** 033302
[39] Miao Y Y, Qiu S, Zhang G P, Wang C K, Ren J F and Hu G C 2021 *Physica E* **131** 114729
[40] Landauer R 1970 *Philos. Mag.* **21** 863
[41] Hu G C, Guo Y, Wei J H and Xie S J 2007 *Phys. Rev. B* **75** 165321
[42] Díez-Pérez I, Hihath J, Lee Y, Yu L P, Adamska L, Kozhushner M A, Oleynik II and Tao N J 2009 *Nat. Chem.* **1** 635
[43] Hu G C, Zhang G P, Ren J F, Wang C K and Xie S J 2011 *Appl. Phys. Lett.* **99** 082105
[44] Hu G C, He K L, Xie S J and Saxena A 2008 *J. Chem. Phys.* **129** 234708
[45] Zhang G P, Hu G C, Song Y, Xie Z and Wang C K 2013 *J. Chem. Phys.* **139** 094702
[46] Taniguchi M, Tsutsui M, Mogi R, Sugawara T, Tsuji Y, Yoshizawa K and Kawai T 2011 *J. Am. Chem. Soc.* **133** 11426
[47] Hong W J, Manrique D Z, Moreno-García P, Gulcur M, Mishchenko A, Lambert C J, Bryce M R and Wandlowski T 2012 *J. Am. Chem. Soc.* **134** 2292
[48] Qiu S, Miao Y Y, Zhang G P, Ren J F, Wang C K and Hu G C 2020 *J. Phys. Chem. C* **124** 12144
[49] Liu X S, Sangtarash S, Reber D, Zhang D, Sadeghi H, Shi J, Xiao Z Y, Hong W J, Lambert C J and Liu S X 2017 *Angew. Chem. Int. Ed.* **129** 179
[50] Guo Y L, Yang C, Zhou S Y, Houk K N and Guo X F 2025 *J. Am. Chem. Soc.* **147** 16972